Valproic Acid Alters Chromatin Structure by Regulation of Chromatin Modulation Proteins

Douglas C. Marchion, Elona Bicaku, Adil I. Daud, Daniel M. Sullivan, and Pamela N. Munster

Department of Interdisciplinary Oncology, Experimental Therapeutics Program, H. Lee Moffitt Cancer Center and Research Institute, Tampa, Florida

Abstract

Histone acetylation and deacetylation are crucial in the regulation of gene expression. Dynamic changes in gene expression may affect chromatin structure and, consequently, the interaction of chromatin with regulatory factors. In this study, the effects of the antiseizure drug valproic acid (VPA) on the expression of genes that regulate the structure of chromatin and the access of macromolecules to the DNA were investigated. Exposure of breast cancer cells to VPA resulted in rapid dose-dependent hyperacetylation of the histones H3 and H4. VPA further induced a depletion of several members of the structural maintenance of chromatin (SMC) proteins, SMC-associated proteins, DNA methyltransferase, and heterochromatin proteins. Down-regulation of these proteins was associated with chromatin decondensation. The observed alterations of chromatin structure correlated with enhanced sensitivity of DNA to nucleases and increased interaction of DNA with intercalating agents. VPA-induced chromatin decondensation led to a sequence-specific potentiation of DNA-damaging agents in cell culture and xenograft models. Modulation of heterochromatin maintenance proteins was not a direct, but a downstream, effect of histone acetylation. The effects on the chromatin structure were reversible upon drug withdrawal, but obligatory for the potentiation of DNA-damaging agents. In addition to their antitumor activity as single agents, the chromatin decondensation induced by histone deacetylase inhibitors may enhance the efficacy of cytotoxic agents that act by targeting DNA. The proposed mechanism of action suggests an effect of drug sequencing on the antitumor activity of these drugs. (Cancer Res 2005; 65(9): 3815-22)

Introduction

Genome stability and transcriptional silencing are accomplished by condensation of the chromatin in the form of heterochromatin. Several genes known to be involved in the maintenance of heterochromatin include the structural maintenance of chromatin (SMC) proteins 1 to 6, SMC-associated proteins, DNA methyltransferase 1 (DNMT1), and heterochromatin protein 1 (HP1). SMC proteins have been classified in six subtypes and function as heterodimer components of large protein complexes that also include several non-SMC proteins. The SMC2-SMC4 and SMC1-SMC3 complexes are also known as condensin and cohesin, respectively. One of their most important roles is chromosome condensation and sister chromatid cohesion. Furthermore, SMC proteins may play a role in DNA recombination and repair pathways (1). Recent studies have suggested that the DNA methyltransferase DNMT1 targets heterochromatin during replication and may be involved in maintaining methylation patterns on newly synthesized DNA (2, 3). DNMT1 may also direct the activity of histone deacetylases (HDAC) to genes that are transcriptionally repressed (4–6) and may interact with HP1 (7). HP1 is involved in gene silencing (8). One model suggests that binding sites for HP1 are generated on histone H3 after histone methylation (9, 10). This suggests that SMC(s), DNMT1, and HP1 work in concert in the epigenetic control of chromatin compaction and gene silencing.

A class of compounds that modulate chromatin dynamics are the HDAC inhibitors. We have previously shown that acetylation of histones by the HDAC inhibitor suberoylanilide hydroxamic acid (SAHA) leads to conformational changes of DNA and chromatin decondensation. SAHA-induced chromatin decondensation was associated with potentiation of DNA damage induced by topo II inhibitors in a sequence-specific manner (11). Similar studies have been reported by others (12). Whereas these studies are important for the clinical development of HDAC inhibitors, they only provided limited insight into a potential mechanism by which the SAHA-induced histone hyperacetylation leads to chromatin decondensation.

Here, we expanded these studies to evaluate the effects of the antiseizure drug valproic acid (VPA, 2-propylpentanoic acid) on histone acetylation and propose a mechanism by which VPA and other HDAC inhibitors may induce chromatin remodeling and promote access of DNA-damaging agents to their target sites. Furthermore, the effects of VPA on the efficacy of DNA-damaging agents were evaluated in a breast cancer xenograft model.

Our data indicate that VPA induced chromatin decondensation in breast cancer cells by repression of SMC 1 to 5 and SMC-associated proteins, DNMT-1, and HP1. VPA-induced chromatin decondensation was associated with an increased sensitivity of DNA to nucleases and increased the association of DNA with intercalating agents. Furthermore, VPA potentiated DNA damage and apoptosis induced by cytotoxic agents that require access to the DNA for activity. VPA led to histone hyperacetylation *in vivo* and *in vitro*. However, unlike the VPA-induced histone hyperacetylation, which was maximal by 1 hour, the regulation of genes involved in chromatin decondensation required prolonged exposure to VPA, suggesting that the modulation of chromatin maintenance proteins are an important additional step in the regulation of chromatin structure. Modulation of heterochromatin maintenance proteins was reversible upon drug withdrawal and was obligatory for potentiation of DNA-damaging agents. Studies in a breast cancer xenograft model indicated that these effects occur at clinically relevant concentrations.

Requests for reprints: Pamela N. Munster, Department of Interdisciplinary Oncology, Experimental Therapeutics Program, H. Lee Moffitt Cancer Center, MRC-4 East 12902 Magnolia Drive, Tampa, FL 33612. Phone: 813-745-8948; Fax: 813-745-1984; E-mail: Munstepn@moffitt.usf.edu.

Materials and Methods

Chemicals and antibodies

VPA and aclarubicin were purchased from Sigma Chemical, Co. (St. Louis, MO) and prepared as a 1 mol/L stock solution. SAHA was provided by Aton Pharma (Tarrytown, NY). Epirubicin was purchased from Pfizer (New York, NY). All other reagents were of analytic grade and purchased from standard suppliers. Antibodies were purchased as follows: acetyl-histone H3 and H4 from Upstate Biotechnology (Waltham, MA); SMC1, SMC3, and HP1 from Chemicon (Temecula, CA); and DNMT1 from Santa Cruz Biotechnology (Santa Cruz, CA).

Cell lines

All cell lines were purchased from American Type Culture Collection (Manassas, VA) and maintained in DMEM with 10% heat-inactivated fetal bovine serum, 2 mmol/L glutamine, and 50 units/mL penicillin and 50 μg/mL streptomycin. For experimental procedures, cells were incubated in a humidified atmosphere with 5% CO_2 at 37°C.

Histone acetylation

Cells were exposed to experimental conditions and acetylated histones were visualized using antiacetylated histone H3 and H4 antibodies by Western blot analysis as described previously (13).

Microarray

Alterations in gene expression induced by VPA were evaluated by microarray using Affymetrix U74Av2 Genechips (900343; Affymetrix Inc., Santa Clara, CA) by standard protocols (Moffitt, Molecular Biology Core). Hybridization to Affymetrix chips was analyzed using Affymetrix Microarray Suite 5.0 software. Signal intensity was scaled to an average intensity of 500 before comparison analysis. The MAS 5.0 software uses a statistical algorithm to assess increases or decreases in mRNA abundance in a direct comparison between two samples (statistical algorithms description document). Two samples of each condition were evaluated and each experiment was repeated at least twice. This analysis is based on the behavior of 16 different oligonucleotide probes designed to detect the same gene. Probe sets that yielded a change in P value of <0.04 were identified as changed (increased or decreased) and those that yielded a P value between 0.04 and 0.06 were identified as marginally changed.

Electron microscopy

Cells were fixed with 4% paraformaldehyde for 1 hour at 37°C. Samples were rinsed with PBS, dehydrated in increasing ethanol concentrations (50%, 70%, 80%, 90%, and 100%), and embedded in water-permeable LR White plastic. Cells were sectioned with a diamond knife at 90 nm thickness and stained for 2 minutes in 1% uranyl acetate and for 5 minutes with lead citrate, and finally examined at 60 kV on a Philips 100M electron microscope at 14,000- and 32,000-fold magnification.

Micrococcal nuclease digestion

MCF-7 cells (1×10^6) were Dounce homogenized in RSB buffer [10 mmol/L Tris-HCl (pH 7.4), 10 mmol/L NaCl, 3 mmol/L $MgCl_2$, 0.5% NP40] containing 10 μg/mL aprotinin and leupeptin, 1 mmol/L phenylmethylsulfonyl fluoride, 1 mmol/L Na_3VO_4, and 1 mmol/L DTT, and incubated on ice for 15 minutes. Samples were washed twice with RSB buffer and digested with 15 units of micrococcal nuclease in digestion buffer [15 mmol/L Tris-HCl (pH 7.5), 60 mmol/L KCl, 15 mmol/L NaCl, 1 mmol/L $CaCl_2$, 3 mmol/L $MgCl_2$, 20% glycerol, 15 mmol/L β-mercaptoethanol] for 5 minutes. Digestion was stopped by adding 1 volume of stop solution [50 mmol/L Tris (pH 7.5), 150 mmol/L NaCl, 50 mmol/L EDTA, 0.3% SDS]. DNA was extracted using 1 volume of phenol/chloroform/isoamyl alcohol (25:24:1) followed by 1 volume chloroform/isoamyl alcohol (24:1) and precipitated with 100% isopropyl alcohol. The DNA was washed once with 70% ethanol, resuspended in Tris-HCl (pH 8.0)/EDTA buffer, and separated using 1.2% agarose gels.

DNase hypersensitivity

Cells (2×10^6) were fixed with 1.5% paraformaldehyde for 15 minutes on ice, washed with cold PBS, and incubated for 16 hours in 70% ethanol at −20°C. Cells were then washed once with PBS and once with ISNT buffer [25 mmol/L $MgCl_2$, 50 mmol/L Tris-HCl (pH 8.0), 10 mmol/L β-mercaptoethanol, 10 μg/mL bovine serum albumin (BSA); ref. 14]. DNA nicks were generated by incubation with 5 units of DNase I in ISNT buffer for 25 minutes. Cells were washed with PBS and incubated in polymerase buffer (16 μmol/L dATP, 16 μmol/L dCTP, 16 μmol/L dGTP, 16 μmol/L dUTP-FITC, 7 units/mL DNA polymerase I) for 90 minutes at 37°C and then analyzed by fluorescence-activated cell sorting (FACS) for the incorporation of dUTP-FITC.

DNA intercalation with acridine orange

MCF-7 cells (2×10^5) were treated with 2 mmol/L VPA for 48 hours and the nuclei purified as described by Nusse et al. (15). Nuclei were exposed to increasing concentrations of acridine orange (0-10 μmol/L) for 10 minutes and fluorescence intensity was measured with the appropriate filter set (excitation 485 nm, emission 535 nm). Similarly, DNA intercalation of epirubicin was measured after cells were exposed for 48 hours to increasing concentrations of VPA followed by a 4-hour epirubicin exposure (1 μmol/L). Fluorescence intensity of epirubicin was assessed as previously described (excitation 485 nm, emission 535 nm; ref. 16).

Comet assay

The alkaline comet assay was done and used according to manufacturer's recommendations (Trevigen, Gaithersburg, MD). Slides were then incubated for 1 hour in alkaline electrophoresis solution (pH > 13). Comet tails were generated by a 40-minute electrophoresis at 20 V, 4°C. Slides were stained for 20 minutes with SYBR green and the comet moment was quantified using the LAI Comet Analysis System.

Evaluation of apoptosis

Apoptosis was scored by the presence of nuclear chromatin condensation and DNA fragmentation and evaluated with fluorescence microscopy using bis-benzimide staining. Cells were fixed in 4% paraformaldehyde for 10 minutes at room temperature and washed with PBS. Cell nuclei were stained with 0.5 μg/mL of bis-benzimide trihydrochloride (Hoechst; Molecular Probes, Eugene, OR). Two hundred cells were counted per experiment in five different fields and scored for apoptosis (nuclei / all nuclei ×100). Each experiment was repeated at least thrice; error bars depict SE.

Clonogenic assays

Cells were treated with 0.5 mmol/L VPA for 48 hours followed by a 4-hour epirubicin exposure. Colonies were evaluated after 14 to 21 days in culture without retreatment, stained with 2% crystal violet in methanol, and counted if measuring at least 0.2 mm. All experiments were repeated at least thrice.

Isobologram analysis

Fractional inhibition of growth was determined using colony-forming assays and isobologram analysis with the CalcuSync software program as described by Chou et al. (17) to determine synergistic, additive, or antagonistic effects from drug combinations. IC_{50}s were calculated as the concentrations required for 50% inhibition of growth.

Animal studies

Four- to six-week old *nu/nu* athymic female mice were obtained from the National Cancer Institute-Frederick Cancer Center (Frederick, MD) and maintained in ventilated caging. Experiments were done under an Institutional Animal Care and Use Committee–approved protocol (R2462) and institutional guidelines for animal welfare. Estrogen pellets (60-day slow release, 0.72 μg, Innovative Research, Sarasota, FL) were placed under the dorsal skin 7 days before tumor inoculation. MCF-7 cells (5×10^6) mixed 1:1 with Matrigel were injected s.c. on the right and left flanks. Once tumors reached 5 mm in the largest diameter, mice were treated in the following cohorts: saline only, VPA only, epirubicin only, and VPA followed by epirubicin. Mice receiving VPA were injected with 500 mg/kg/d VPA in 0.1 mL saline i.p. twice daily for 5 doses. Epirubicin (3 mg/kg in 0.1 mL saline) was injected once after the last dose of VPA. The respective control groups received corresponding saline injections.

Tumor growth. Tumor growth (four to eight mice per cohort) was monitored three to four times per week by measuring two perpendicular

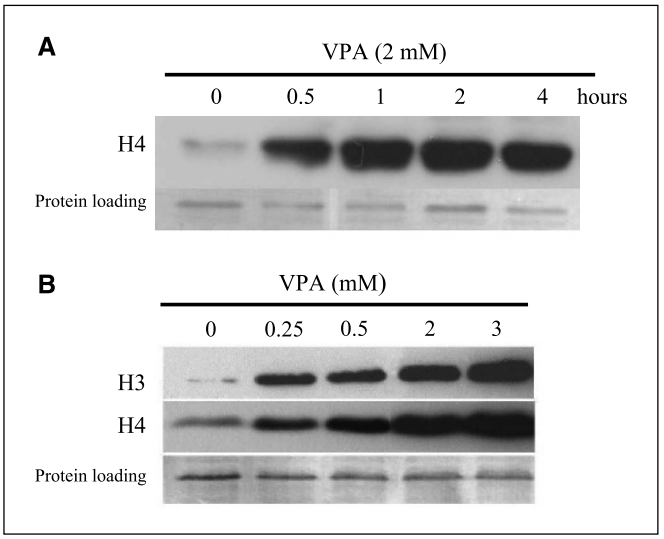

Figure 1. VPA-induced histone acetylation. *A,* acetylation of histone H4 determined by Western blot analysis of MCF-7 cells treated with 2 mmol/L VPA for 0, 0.5, 1, 2, and 4 hours. *B,* acetylation of histones H3 and H4 in MCF-7 cells in response to a 48-hour exposure of 0, 0.25, 0.5, 2, or 3 mmol/L VPA.

tumor diameters with a caliper. Tumor volumes were calculated as $V = \pi / 6 \times \text{length} \times \text{width}^2$. Animals were sacrificed when the largest tumor diameter reached 13 mm. Statistical analysis was done using paired Student's t test and multivariate analysis by ANOVA for comparisons within and among groups.

Histone acetylation. Tumor cells isolated from mice (three mice per experimental group) injected with saline or 500 mg/kg/d VPA for 48 hours were evaluated for histone H3 acetylation by immunofluorescence. Briefly, tumors were dissected with care taken to remove the extraneous connective tissue. Tumors were minced in 1 mL PBS containing 200 units of type III collagenase and incubated for at 37°C for 1 hour. Single cells were acquired by passage through a 35 μm nylon mess. Cells were washed in PBS, adhered to glass slides using Cytospin Funnels, and fixed with 95% ethanol, 5% acetic acid for 1 minute. Slides were then incubated with antiacetylated H3 antibody in 2% BSA for 1 hour, washed, and then incubated with fluorescent-labeled secondary antibody for 1 hour and nuclei were counterstained with 0.5 μg/mL bis-benzimide (Hoechst). Images were acquired by confocal microscopy acquired as TIFF files, and H3 staining was analyzed for square pixel surface area. Statistical analysis was done by Student's t test.

Results

The effects of valproic acid on histone acetylation and cell growth. Several studies have suggested that treatment of cells with VPA results in histone hyperacetylation, growth arrest, and cell differentiation in several tumor cell lines (18–23). We found that VPA induced maximal histone H4 acetylation as early as 1 hour (Fig. 1*A*) and occurred at concentrations of VPA as low as 0.25 mmol/L (Fig. 1*B*). Similar findings were observed for histone H3 (Fig. 1*B*). As reported by others, the IC_{50}s for HDAC 1 to 5 inhibition ranged from 0.7 to 1.5 mmol/L VPA (24). We found that in MCF-7 cells, the IC_{50} for growth arrest was 1.35 mmol/L (95% confidence interval, 1.21-1.50 mmol/L). Growth arrest was associated with an accumulation of cells in G_1. The IC_{95} was 7.6 mmol/L (95% confidence interval, 6.73-8.53). The IC_{50}s for this breast cancer cell line were similar to other breast cancer cells, such as SKBr-3, BT-474, and MDA-361 (data not shown).

Valproic acid induces down-regulation of proteins essential for the maintenance of chromatin. Several lines of evidence suggest that SMCs, DNMT1, and HP1 work in concert in the epigenetic control of chromatin compaction and gene silencing. Histone acetylation is believed to be associated with a direct physical dissociation of the histone:DNA complex as well as downstream effects on gene transcription by either inhibiting histone binding of transcription factors or regulation of coactivators and repressors (25). We have shown that maximal histone acetylation occurred by 1 hour. We then evaluated the effects of VPA on the expression of proteins that are involved in the maintenance and dynamics of heterochromatin. Treatment of cells with VPA resulted in a decrease in the mRNA levels of SMC proteins, SMC-associated proteins, DNMT1, and HP1 by microarray analysis (Fig. 2*A*). However, unlike histone acetylation, a 48-hour exposure to VPA was required to achieve a >50% reduction in mRNA expression of these chromatin regulators. The decrease in the expression of these genes conferred a depletion of the effector proteins after treatment with 2 mmol/L VPA for 48 hours (data not shown; Fig. 2*B*). Shorter exposure did not affect protein expression (data not shown). A depletion of these proteins was also observed with prolonged exposure to another HDAC inhibitor, SAHA (Fig. 2*B*). These findings suggest that the decrease in mRNA expression is more likely due to a transcriptional regulation of these genes because of HDAC inhibition rather than a direct VPA effect.

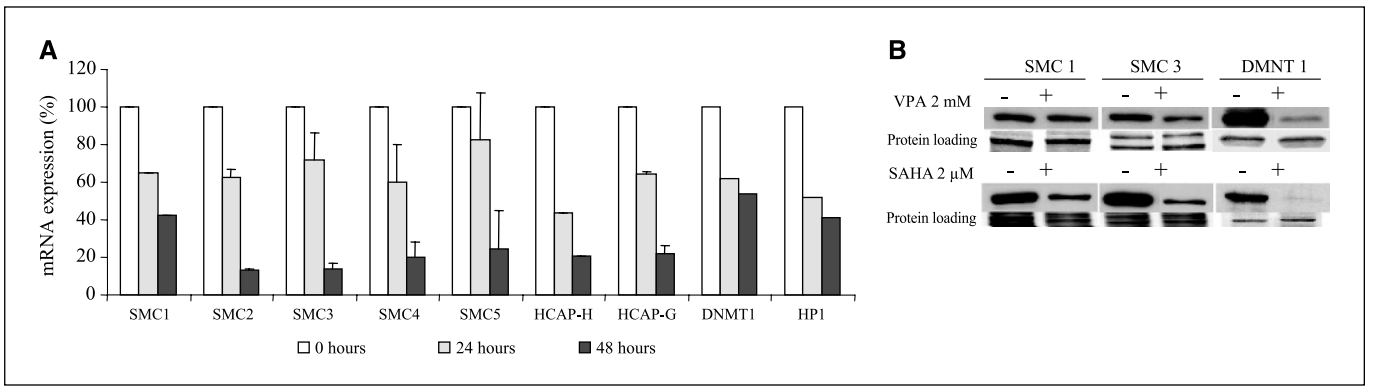

Figure 2. VPA-induced down-regulation of proteins involved in the maintenance of heterochromatin. *A,* changes in mRNA expression by microarray analysis of SMC 1 to 5 proteins, SMC-associated proteins, HCAP-H and HCAP-G, DNMT1, and HP1 after a 48-hour exposure to 2 mmol/L VPA. *Bars,* SE. *B,* changes in protein expression of SMC 1, SMC 3, and DMNT 1 by Western blot analysis after a 48-hour exposure to 2 mmol/L VPA or 2 μmol/L SAHA.

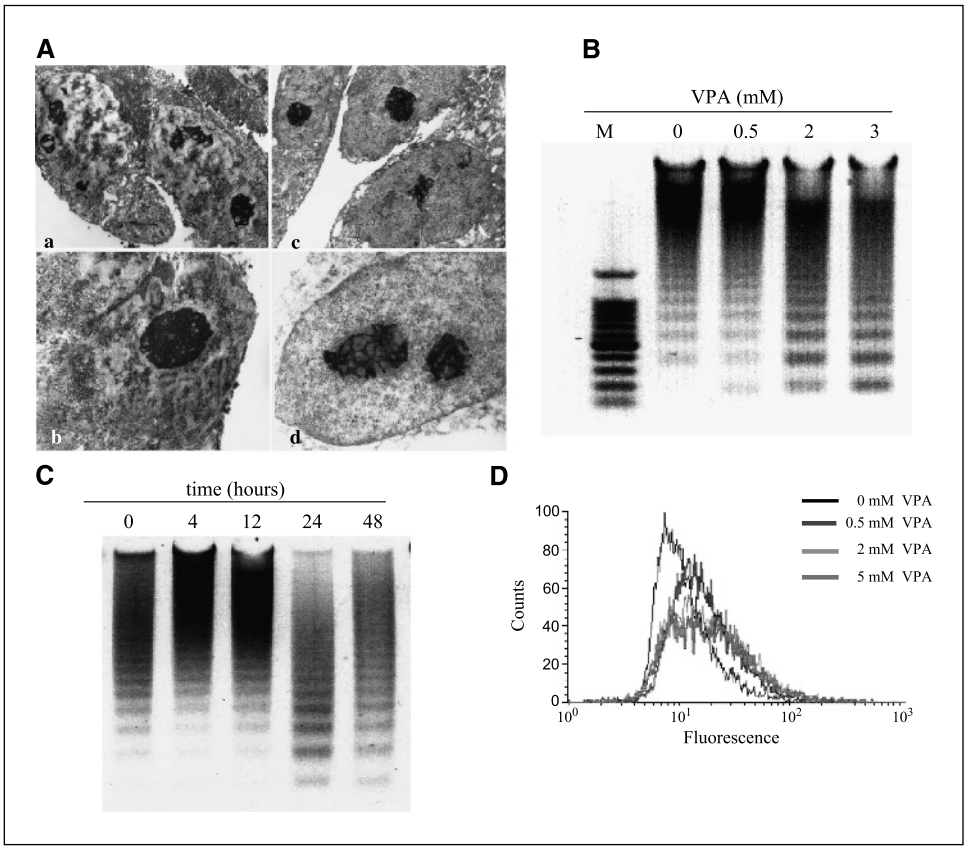

Figure 3. VPA-induced changes in chromatin structure. *A,* electron microscopy analysis of MCF-7 cells treated with 0 or 0.5 mmol/L VPA for 48 hours. Untreated cells displayed dense nucleoli and condensed pattern of heterochromatin (*a,* ×14,000; *b,* ×32,000). In contrast, cells treated with 2 mmol/L VPA for 48 hours showed an even dispersion of the chromatin (*c,* ×14,000; *d,* ×32,000). Micrococcal nuclease digestion of MCF-7 cell DNA after treatment with 0, 0.5, 2, and 3 mmol/L VPA for 48 hours (*B*) and with 2 mmol/L VPA for 0, 4, 12, 24, and 48 hours (*C*). *D, in situ* nick translation of MCF-7 cells treated with 0, 0.5, 2, and 5 mmol/L VPA for 48 hours and analyzed by FACS. The mean fluorescence intensity ± SD of untreated cells was 7.8 ± 2.3. In contrast, treated cells showed a shift in fluorescence intensity as follows: 0.5 mmol/L, 12.8 ± 2.3; 2 mmol/L, 13.9 ± 3.0; 5 mmol/L, 16.0 ± 0.51, $P < 0.05$ for treated versus untreated groups.

The effects of valproic acid on chromatin structure. To determine if the VPA-induced transcriptional repression of SMC(s), SMC-associated proteins, DNMT1, and HP1 resulted in chromatin decondensation, we assessed VPA-induced changes in the chromatin structure by electron microscopy. Figure 3*A-a* shows untreated tumor cells at a ×14,000 magnification. The nuclei of these cells revealed dense nucleoli and a condensed pattern of heterochromatin evenly dispersed in the nuclei. Figure 3*A-b* is an enlargement of one of the nuclei from an untreated MCF-7 cell (×32,000). Figure 3*A-c* (×14,000) and *A-d* (×32,000) shows cells treated with 0.5 mmol/L VPA for 48 hours. In contrast to untreated cells, VPA treatment resulted in a prominent change in the distribution of heterochromatin, causing the chromatin to disperse evenly. As described above, VPA-induced histone hyperacetylation was maximal after 1 hour. If VPA-induced chromatin decondensation were a direct effect of changes in electrostatic interaction due to histone acetylation, alterations in the chromatin structure should be observed rapidly. However, prominent changes in chromatin structure required a 48-hour exposure to VPA (data not shown) and correlated with depletion of the SMC proteins. For a more quantitative assessment of the time and dose dependence of VPA-induced chromatin decondensation, we evaluated the susceptibility of DNA to nucleases. MCF-7 cells were treated with increasing concentrations of VPA and exposed to micrococcal nuclease. The resulting DNA fragments in VPA-treated samples displayed the characteristic nucleosomal ladder (Fig. 3*B*) suggestive of chromatin decondensation. A digest of cells treated with 2 and 3 mmol/L VPA produced mostly mono-, di-, and trinucleosomal fragments compared with cells treated without VPA. Mono- and dinucleosomal fragments were also detected in cells treated with 0.5 mmol/L VPA, but to a lesser degree. Time course of DNA digestion showed that a notable increase in the small fragments were not detected until 24 hours of VPA exposure (Fig. 3*C*), suggesting that chromatin decondensation was a late effect unlike histone acetylation which peaked as early as 1 hour after VPA exposure. VPA-induced chromatin decondensation was also tested by determining the sensitivity of DNA to DNase I using *in situ* nick translation. As shown in Fig. 3*D*, MCF-7 cells exposed to VPA showed a shift in the fluorescence intensity, suggesting an increase in DNA vulnerability to DNase I. The median fluorescence intensity of untreated and VPA-treated cells were as follows: VPA 0 mmol/L, 7.8 (±2.3); 0.5 mmol/L, 12.8 (±2.3); 2 mmol/L, 13.9 (±3.0); and 5 mmol/L, 16.0 (±0.51), $P < 0.05$ for treated cells compared with untreated cells.

Preexposure to valproic acid results in increased access of DNA to intercalating agents. To determine if VPA-induced chromatin decondensation increased the access of DNA to macromolecules, we evaluated the association of chromatin with the DNA-intercalating agent dye, acridine orange. Acridine orange has well-known spectral and self-aggregation characteristics. It intercalates into double-stranded DNA and produces green fluorescence with a maximal emission at 526 nm. Interference of acridine orange interaction with RNA was eliminated by RNase digestion. As seen in Fig. 4*A*, preexposure to VPA resulted in a linear increase in the DNA intercalation of acridine orange, suggesting that the DNA was more accessible to the dye. Similarly, a 48-hour preexposure of cells to increasing concentrations of VPA increased the DNA binding of epirubicin, a cytotoxic anticancer agent used for the treatment of breast cancer (Fig. 4*B*).

Valproic acid–induced chromatin decondensation results in increased DNA damage induced by cytotoxic agents *in vitro*. To determine if increased access of macromolecules to chromatin increased the cytotoxicity of DNA-damaging agents, epirubicin-induced DNA strand breaks were measured after preexposure to VPA by comet assay as described in Materials and Methods. MCF-7 cells were treated with 0 or 2 mmol/L VPA for 48 hours and then exposed to 1 μmol/L epirubicin. The comet moments were as follows: control, 0 (±0.4); VPA alone, 2.5 (±0.7); epirubicin alone, 9.9 (±1.1); or VPA → epirubicin, 32.3 (±3.1), $P < 0.05$; these results suggest that epirubicin-induced comet moments were significantly increased in the presence of VPA. To determine if the potentiation of anthracycline-induced DNA damage by VPA translated into cell death, epirubicin- and aclarubicin-induced apoptosis were assessed in the presence of VPA. MCF-7 cells were treated with VPA for 48, 24, 12, 4, or 0 hours before being exposed to an anthracycline (Fig. 5*A*). Potentiation of epirubicin- and aclarubicin-induced apoptosis was only observed after prolonged VPA preexposure (48 hours) and was abrogated with shorter preexposure or when concomitantly treated. VPA-induced potentiation of epirubicin was also evaluated by clonogenic assays. As depicted by the fractional inhibition, cells treated with 0.5 mmol/L VPA before epirubicin showed a decrease in survival when compared with cells treated with epirubicin alone (Fig. 5*B*). Isobologram analysis indicated that the combination was synergistic across all dose levels tested (Fig. 5*C*).

Recovery of heterochromatin maintenance proteins results in abrogation of potentiation. We have previously reported that the HDAC inhibitor SAHA induced growth arrest and differentiation in breast cancer cells (13). These effects required continuous presence of the drug and were reversible upon withdrawal of SAHA. To determine if the effects of VPA on chromatin structure were reversible, MCF-7 cells were treated with 2 mmol/L VPA for 48 hours. VPA was then replaced with media, and protein expression of heterochromatin maintenance proteins was analyzed after a 2-, 4-, 8-, 24-, and 48-hour washout period by Western blot analysis (Fig. 5*D*). VPA treatment of cells for 48 hours resulted in the depletion of SMC3, DNMT1, and HP1 (Fig. 2*B* and 5*D*). These depleted proteins were recovered to levels comparable with untreated cells within 48 hours after the removal of VPA, indicating that the VPA effects were reversible. As shown in Fig. 5*E*, recovery of these depleted proteins resulted in an abrogation of synergy between VPA and epirubicin. MCF-7 cells were exposed to VPA either for 96 hours (48-48), for 48 hours of vehicle followed by 48 hours of VPA (0-48), or for 48 hours of VPA followed by a washout period of 48 hours of vehicle (48-0). The cells were then treated with epirubicin for 4 hours and assessed for apoptosis for 24 hours. As shown in Fig. 5*E*, 48-hour pretreatment with VPA showed significant potentiation of epirubicin-induced apoptosis, which was not further increased by preexposure time of 96 hours. However, VPA-induced sensitization to epirubicin was abrogated when cells were exposed to VPA for 48 hours followed by a 48-hour washout period before epirubicin exposure. These findings suggest that the effects of the HDAC inhibitors are reversible and that attention has to be given to adequate dosing and scheduling to ensure that the effects of HDAC inhibition are maintained at the time of epirubicin exposure.

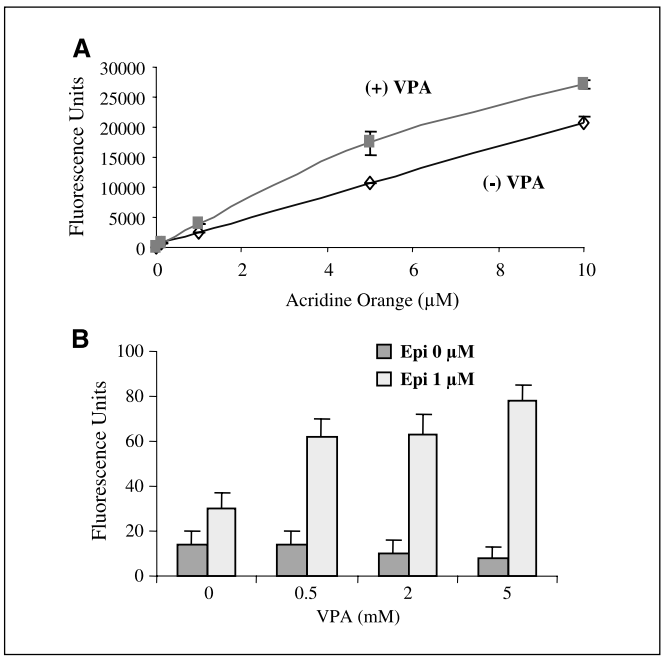

Figure 4. VPA increases the association of intercalating agents with DNA. Evaluation of fluorescence intensity of acridine orange (*A*) and epirubicin (*B*) in MCF-7 cells treated with 0 or 2 mmol/L VPA for 48 hours. Preexposure of cells to VPA was associated with increased DNA binding of acridine orange and epirubicin (*Epi*) to DNA.

Valproic acid–induced histone acetylation and chromatin decondensation in a breast cancer xenograft model. To determine if the effects of VPA on cancer cell lines are reproducible in an *in vivo* model, we evaluated histone acetylation and tumor growth in a breast cancer xenograft model. Mice bearing MCF-7 tumors were treated with 0 or 500 mg/kg/d VPA twice a day for 48 hours. Tumor cells were isolated 4 hours after the last dose of VPA and assayed for acetylated histone H3 by immunofluorescence as described in Materials and Methods. Tumor cells isolated from mice treated with VPA showed a 2.7-fold increase in the square pixel surface area of acetylated histone H3 staining when compared with controls (Fig. 6*A*). VPA potentiated the antitumor effects of epirubicin in this xenograft model. As shown in Fig. 6*B*, tumor progression was significantly inhibited ($P < 0.05$) in animals treated with VPA followed by epirubicin compared with mice treated with saline, epirubicin, or VPA alone. The concentration of VPA used in this study reflects plasma concentrations of ~3 mmol/L (26, 27). VPA plasma concentrations typically used for the chronic treatment of migraine headaches or seizures range from 0.3 to 1.1 mmol/L [Food and Drug Administration (FDA) package insert]. Higher concentrations are achievable for shorter exposure times without significant toxicities.[1]

Discussion

This study reports the effects of VPA on chromatin structure and dynamics in breast cancer cells. VPA has been in clinical use for over 35 years for the treatment of seizures, mood disorders, and lately for migraine headaches. Recent studies have indicated that VPA may also have anticancer activity against a variety of tumor types (18–22, 28, 29). Similar to those studies, our results showed a

[1] Unpublished data from ongoing clinical trial (MCC13693, IRB101881) and FDA package insert.

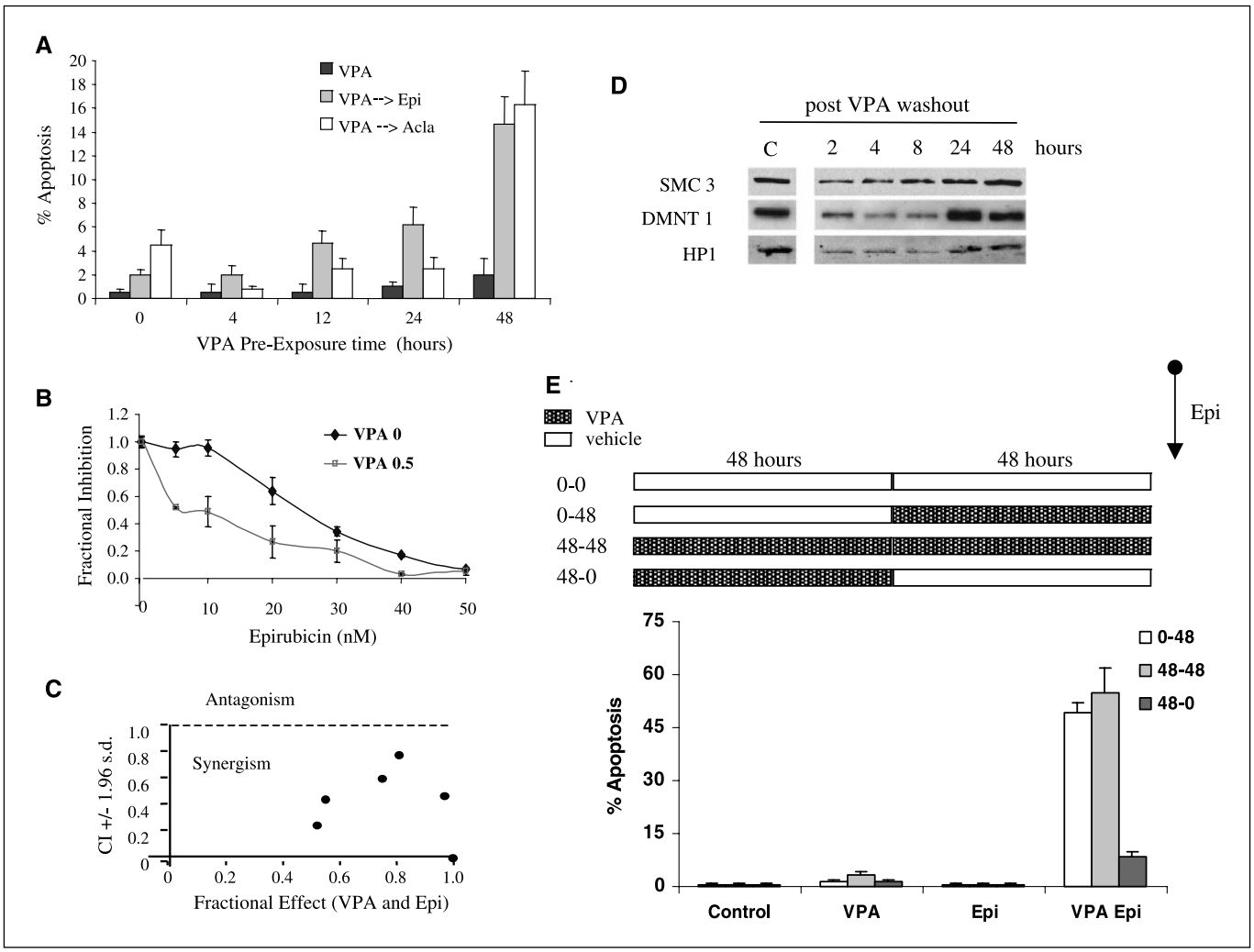

Figure 5. Prolonged exposure to VPA potentiated the apoptosis induced by cytotoxic antitumor agents. *A,* evaluation of apoptosis by nuclear fragmentation in MCF-7 cells treated with 2 mmol/L VPA for 0, 4, 12, 24, and 48 hours followed by the anthracyclines, epirubicin or aclarubicin (*Acla*), for 4 hours. Statistical analysis by Student's *t* test and ANOVA showed that only 48-hour preexposure to 2 mmol/L VPA compared with epirubicin or aclarubicin treatment alone was associated with a significant increase in apoptosis (*VPA* → *Epi*, $P = 0.0009$) and aclarubicin (*VPA* → *Acla*, $P = 0.003$). *B,* colony formation of MCF-7 cells by clonogenic assays in the presence of 0.5 mmol/L VPA. Cells treated with VPA for 48 hours before epirubicin showed a decrease in survival compared with cells treated with epirubicin alone. *C,* isobologram analysis of the clonogenic assays indicated a synergistic enhancement of epirubicin-induced cell growth inhibition by VPA. *D,* VPA-induced effects on protein expression of SMC3 and HP1 proteins in MCF-7 cells treated with VPA for 48 hours followed by a 2-, 4-, 8-, 24-, and 48-hour washout period by Western blot analysis. VPA-depleted proteins were recovered to levels comparable with untreated cells within 48 hours after the removal of VPA. *E,* reversibility of VPA-induced potentiation of epirubicin-induced apoptosis. MCF-7 cells were exposed to VPA either for 96 hours (48-48), for 48 hours of vehicle followed by 48 hours of VPA (0-48), or for 48 hours of VPA followed by a washout period of 48 hours (48-0). The cells were then treated with epirubicin for 4 hours and assessed for apoptosis 24 hours. Recovery of VPA-depleted proteins during the washout period resulted in abrogation of synergy between VPA and epirubicin. VPA exposure beyond 48 hours did not further potentiate epirubicin-induced apoptosis.

VPA-induced growth arrest in several breast cancer cell lines. However, we found that when given as a single agent, VPA resulted in a reversible cell cycle arrest and caused only a low degree of apoptosis.

VPA has been reported to function as an HDAC inhibitor, leading to the acetylation of histone tails (23, 30). Histone acetylation results in attenuation of the electrostatic charge interactions between histones and DNA and has been associated with chromatin decondensation (11, 12, 31). However, other studies postulate that histone acetylation alone may have minimal effects on chromatin structure (32). Epigenetic silencing is accomplished by condensation of the chromatin in the form of heterochromatin and has been associated with hypoacetylation and hypermethylation. Furthermore, the expression of proteins involved in the maintenance of heterochromatin, such as the SMC proteins, SMC-associated proteins, DNMT1, and HP1, affects the dynamics of the chromatin structure. As reported in other cell systems (18–23, 28–30), we observed a rapid, but reversible, histone hyperacetylation in the examined breast cancer cells and the MCF-7 xenograft model with clinically relevant concentrations of VPA. In the cultured cells, the maximal effects occurred by 1 hour of exposure (Fig. 1*A*). In addition, we found that VPA caused a decrease in the expression of mRNA encoding SMC proteins 1 to 5, several SMC-associated proteins, DNMT1, and HP1 (Fig. 2*A*) with subsequent depletion of the corresponding proteins (Fig. 2*B*). Whereas our data is most consistent with a transcriptional regulation of these genes, the possibility that VPA and SAHA may decrease the stability of mRNA transcripts

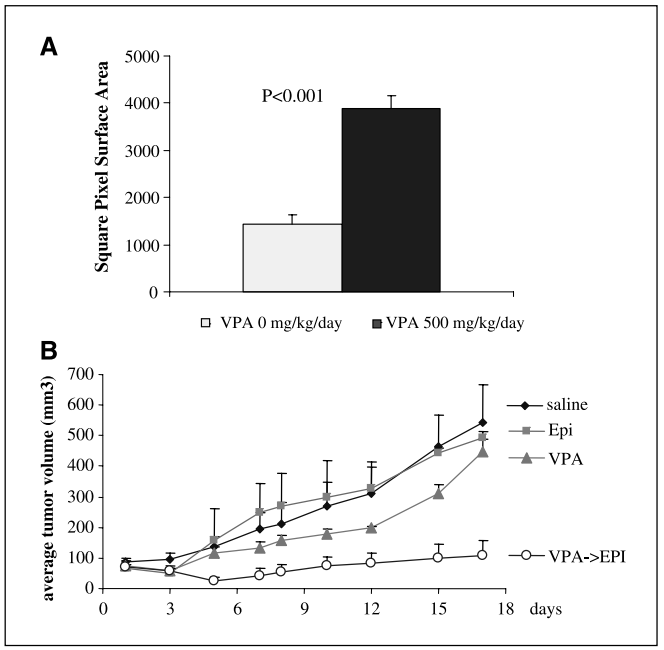

Figure 6. VPA-induced histone acetylation and potentiation of epirubicin in a MCF-7 breast cancer xenograft model. *A,* acetylation of histone H3 in MCF-7 cells isolated from tumors of mice treated with either 0 or 500 mg/kg/d VPA for 48-hour (three mice per cohort). Analysis of square pixel surface area showed a 2.7-fold increase in the H3 acetylation in VPA-treated mice ($P < 0.001$). *B,* VPA potentiated the epirubicin-induced inhibition of tumor growth. Tumor-bearing mice (four to eight mice) received i.p. injections of either saline or 500 mg/kg/d given twice a day for five doses followed by one i.p. injection of either saline or epirubicin (3 mg/kg/d × 1). Cycles were repeated once every week for three cycles. The cohorts were as follows: saline (♦), VPA alone (▲), epirubicin alone (■), or VPA followed by epirubicin (○). Tumor growth was significantly inhibited ($P > 0.05$) in animals treated with VPA followed by epirubicin compared with all other treatments.

or target them for proteasomal degradation cannot be entirely ruled out.

Down-regulation of these proteins resulted in profound changes in the chromatin structure as determined by electron microscopy (Fig. 3*A*). These chromatin structure changes correlated with increased sensitivity of DNA to nucleases, further indicating decondensation of the chromatin (Fig. 3*B-D*). Whereas we observed maximal histone acetylation within 1 hour at concentration of VPA as low 0.25 mmol/L (Fig. 1*A* and *B*), chromatin decondensation required higher concentrations of VPA as well as longer exposure times (at least 24-48 hours; Fig. 3). The kinetics and concentrations of VPA required to induce changes in the chromatin structure imply that the attenuation of electrostatic charges between DNA and histones induced by hyperacetylation of histones is not sufficient to explain chromatin decondensation. The results of this study indicate that the VPA-induced modulation of heterochromatin maintenance proteins is an important additional step in the control of the chromatin structure and its access to regulatory factors. Chromatin decondensation was also seen with other HDAC inhibitors, such as SAHA (11), arguing against a selective or direct effect of VPA.

VPA-induced chromatin decondensation led to enhanced sensitivity of DNA to nucleases and increased DNA binding by intercalating agents (Fig. 4*A* and *C*), signifying an increase in the access of macromolecules to DNA. This is supported by our data showing an increase in epirubicin binding to DNA and a potentiation of epirubicin- and aclarubicin-induced apoptosis and inhibition of colony growth after preexposure to VPA, which followed the kinetics of VPA-induced chromatin decondensation (Fig. 5*A* and *B*). Synergy, as determined by isobologram analysis (Fig. 5*C*) between epirubicin and VPA, was only observed when cells were preexposed to VPA for 48 hours. Short preexposure time or concomitant exposure abrogated this synergy. We have shown earlier that the effects of the HDAC inhibitor SAHA on tumor cell growth and differentiation were reversible and required the continuous presence of drug for biological effects (13). This is supported by the clinical evaluation of SAHA, where benefits were only observed when the drug was administered at least 3 to 5 d/wk (ref. 33 and Cancer Therapy Evaluation Program solicitation letter). The effects of VPA on tumor cells were reversible. Within 2 hours of VPA withdrawal, histone hyperacetylation was reversed; within 48 hours, the depleted chromatin structural proteins had reverted to baseline levels (Fig. 5*D*). In addition, the synergy between VPA and epirubicin was abrogated when VPA was washed out for 48 hours before epirubicin exposure (Fig. 5*E*). Whereas the VPA effects on the structural maintenance proteins are obligatory at the time of epirubicin exposure for synergy, a 48-hour preexposure seems to be optimal as the VPA pretreatment duration. Exposure of cells beyond 96 hours maintained the synergistic effects without further benefits (Fig. 5*E*). The latter findings are not consistent with an outgrowth of resistant cells, as one would expect an abrogation of synergy if the resistant cells were outnumbering the sensitive cells. The reversibility of HDAC inhibitor may pose limitations on their use as anticancer agents and may emphasize a more important role in sensitizing cells to cytotoxic agents.

The effects of VPA on tumor cell lines were then evaluated *in vivo* using a breast cancer xenograft model. Similar to *in vitro* experiments, treatment of tumor-bearing mice resulted in histone acetylation of tumor cells (Fig. 6*A*). Furthermore, we showed that a 48-hour treatment of mice with VPA-sensitized tumors to epirubicin induced growth inhibition *in vivo* (Fig. 6*B*) at concentrations where either drug alone had very little effect on tumor growth. Both drugs were used at concentrations relevant for clinical use and a clinical trial of this sequence-specific combination is currently ongoing.

In summary, we showed that VPA-induced chromatin decondensation correlated with transcriptional repression of gene and proteins involved in the maintenance of heterochromatin and the control of DNA access. The dose and duration of VPA required to induce changes in the chromatin structure indicate that the attenuation of DNA-histone charge interaction due to VPA-induced histone acetylation is not sufficient for chromatin decondensation, but rather a downstream effect of HDAC inhibition. We propose that the VPA-induced modulation of the chromatin structural proteins rather than histone hyperacetylation results in chromatin decondensation. VPA-induced chromatin decondensation may enhance the activity of targeting agents that depend on access to the target site.

These findings have several clinical implications: Histone hyperacetylation is a rapid event and may occur at lower concentrations than those required for chromatin decondensation. Hence, histone hyperacetylation may not be a reliable predictive surrogate or even pharmacologic marker of HDAC inhibitor when used as antitumor agents. The effects of VPA on chromatin

structure were reversible, but obligatory for the potentiation of epirubicin-induced DNA damage. Therefore, maximal benefits in combinations between HDAC inhibitor and DNA-damaging agents are likely schedule dependent and may necessitate higher drug concentrations than those observed for histone acetylation. Moreover, the VPA-induced modulation of the chromatin structure proteins may be an alternative surrogate when evaluating HDAC inhibitors in translational studies.

Acknowledgments

Received 7/15/2004; revised 11/15/2004; accepted 1/13/2005.

Grant support: American Cancer Society Florida F02F-USF-1, Don Shula Foundation, Susan G. Komen Breast Cancer Foundation, and Molecular Oncology Program Project CA 82533.

The costs of publication of this article were defrayed in part by the payment of page charges. This article must therefore be hereby marked *advertisement* in accordance with 18 U.S.C. Section 1734 solely to indicate this fact.

We thank Dr. Nikola Valkov for his assistance with the electron micrographs and Joel Turner for his assistance with the micrococcal nuclease.

References

1. Strunnikov AV, Jessberger R. Structural maintenance of chromosomes (SMC) proteins: conserved molecular properties for multiple biological functions. Eur J Biochem 1999;263:6–13.
2. Pradhan S, Bacolla A, Wells RD, Roberts RJ. Recombinant human DNA (cytosine-5) methyltransferase. I. Expression, purification, and comparison of *de novo* and maintenance methylation. J Biol Chem 1999;274:33002–10.
3. Rountree MR, Bachman KE, Baylin SB. DNMT1 binds HDAC2 and a new co-repressor, DMAP1, to form a complex at replication foci. Nat Genet 2000;25:269–77.
4. Bachman KE, Rountree MR, Baylin SB. Dnmt3a and Dnmt3b are transcriptional repressors that exhibit unique localization properties to heterochromatin. J Biol Chem 2001;276:32282–7.
5. Fuks F, Burgers WA, Brehm A, Hughes-Davies L, Kouzarides T. DNA methyltransferase Dnmt1 associates with histone deacetylase activity. Nat Genet 2000;24:88–91.
6. Fuks F, Burgers WA, Godin N, Kasai M, Kouzarides T. Dnmt3a binds deacetylases and is recruited by a sequence-specific repressor to silence transcription. EMBO J 2001;20:2536–44.
7. Fuks F, Hurd PJ, Deplus R, Kouzarides T. The DNA methyltransferases associate with HP1 and the SUV39H1 histone methyltransferase. Nucleic Acids Res 2003;31:2305–12.
8. Jones DO, Cowell IG, Singh PB. Mammalian chromodomain proteins: their role in genome organisation and expression. Bioessays 2000;22:124–37.
9. Peters AH, O'Carroll D, Scherthan H, et al. Loss of the Suv39h histone methyltransferases impairs mammalian heterochromatin and genome stability. Cell 2001;107:323–37.
10. Piacentini L, Fanti L, Berloco M, Perrini B, Pimpinelli S. Heterochromatin protein 1 (HP1) is associated with induced gene expression in *Drosophila* euchromatin. J Cell Biol 2003;161:707–14.
11. Marchion DC, Bicaku E, Daud AI, Richon V, Sullivan DM, Munster PN. Sequence-specific potentiation of topoisomerase II inhibitors by the histone deacetylase inhibitor suberoylanilide hydroxamic acid. J Cell Biochem 2004;92:223–37.
12. Kim MS, Blake M, Baek JH, Kohlhagen G, Pommier Y, Carrier F. Inhibition of histone deacetylase increases cytotoxicity to anticancer drugs targeting DNA. Cancer Res 2003;63:7291–300.
13. Munster PN, Troso-Sandoval T, Rosen N, Rifkind R, Marks PA, Richon VM. The histone deacetylase inhibitor suberoylanilide hydroxamic acid induces differentiation of human breast cancer cells. Cancer Res 2001;61:8492–7.
14. Jones CB, McIntosh J, Huang H, Graytock A, Hoyt DG. Regulation of bleomycin-induced DNA breakage and chromatin structure in lung endothelial cells by integrins and poly(ADP-ribose) polymerase. Mol Pharmacol 2001;59:69–75.
15. Nusse M, Beisker W, Hoffmann C, Tarnok A. Flow cytometric analysis of G_1- and G_2/M-phase subpopulations in mammalian cell nuclei using side scatter and DNA content measurements. Cytometry 1990;11:813–21.
16. Zhou Q, Chowbay B. Determination of doxorubicin and its metabolites in rat serum and bile by LC: application to preclinical pharmacokinetic studies. J Pharm Biomed Anal 2002;30:1063–74.
17. Chou TC, Motzer RJ, Tong Y, Bosl GJ. Computerized quantitation of synergism and antagonism of taxol, topotecan, and cisplatin against human teratocarcinoma cell growth: a rational approach to clinical protocol design. J Natl Cancer Inst 1994;86:1517–24.
18. Kawagoe R, Kawagoe H, Sano K. Valproic acid induces apoptosis in human leukemia cells by stimulating both caspase-dependent and -independent apoptotic signaling pathways. Leuk Res 2002;26:495–502.
19. Blaheta RA, Cinatl J Jr. Anti-tumor mechanisms of valproate: a novel role for an old drug. Med Res Rev 2002;22:492–511.
20. Knupfer MM, Hernaiz-Driever P, Poppenborg H, Wolff JE, Cinatl J. Valproic acid inhibits proliferation and changes expression of CD44 and CD56 of malignant glioma cells *in vitro*. Anticancer Res 1998;18:3585–9.
21. Driever PH, Knupfer MM, Cinatl J, Wolff JE. Valproic acid for the treatment of pediatric malignant glioma. Klin Padiatr 1999;211:323–8.
22. Cinatl J Jr, Cinatl J, Driever PH, et al. Sodium valproate inhibits *in vivo* growth of human neuroblastoma cells. Anticancer Drugs 1997;8:958–63.
23. Gottlicher M, Minucci S, Zhu P, et al. Valproic acid defines a novel class of HDAC inhibitors inducing differentiation of transformed cells. EMBO J 2001;20:6969–78.
24. Gurvich N, Tsygankova OM, Meinkoth JL, Klein PS. Histone deacetylase is a target of valproic acid-mediated cellular differentiation. Cancer Res 2004;64:1079–86.
25. Cress WD, Seto E. Histone deacetylases, transcriptional control, and cancer. J Cell Physiol 2000;184:1–16.
26. Roma-Giannikou E, Syriopoulou V, Kairis M, Pangali A, Sarafidou J, Constantopoulos A. *In vivo* effect of sodium valproate on mouse liver. Cell Mol Life Sci 1999;56:363–9.
27. Borowicz KK, Sekowski A, Drelewska E, Czuczwar SJ. Riluzole enhances the anti-seizure action of conventional antiepileptic drugs against pentetrazole-induced convulsions in mice. Pol J Pharmacol 2004;56:187–93.
28. Zhu WG, Otterson GA. The interaction of histone deacetylase inhibitors and DNA methyltransferase inhibitors in the treatment of human cancer cells. Curr Med Chem Anti-Canc Agents 2003;3:187–99.
29. Cinatl J Jr, Kotchetkov R, Blaheta R, Driever PH, Vogel JU, Cinatl J. Induction of differentiation and suppression of malignant phenotype of human neuroblastoma BE(2)-C cells by valproic acid: enhancement by combination with interferon-α. Int J Oncol 2002;20:97–106.
30. Phiel CJ, Zhang F, Huang EY, Guenther MG, Lazar MA, Klein PS. Histone deacetylase is a direct target of valproic acid, a potent anticonvulsant, mood stabilizer, and teratogen. J Biol Chem 2001;276:36734–41.
31. Garcia-Ramirez M, Rocchini C, Ausio J. Modulation of chromatin folding by histone acetylation. J Biol Chem 1995;270:17923–8.
32. Lutter LC, Judis L, Paretti RF. Effects of histone acetylation on chromatin topology *in vivo*. Mol Cell Biol 1992;12:5004–14.
33. Kelly WK, Richon VM, O'Connor O, et al. Phase I clinical trial of histone deacetylase inhibitor: suberoylanilide hydroxamic acid administered intravenously. Clin Cancer Res 2003;9:3578–88.

Valproic Acid Alters Chromatin Structure by Regulation of Chromatin Modulation Proteins

Douglas C. Marchion, Elona Bicaku, Adil I. Daud, et al.

Cancer Res 2005;65:3815-3822.